DOI: 10.1002/chem.201100975

Rose Bengal-Grafted Biodegradable Microcapsules: Singlet-Oxygen Generation and Cancer-Cell Incapacitation

Xiao-Lei Wang,[a] Yu Zeng,[a] Yan-Zhen Zheng,[a] Jian-Feng Chen,[b] Xia Tao,*[a] Ling-Xuan Wang,[c] and Yan Teng[d]

Abstract: Rose bengal-grafted chitosan (RB-CHI), synthesized through dehydration between amino and carboxyl functional groups under mild conditions, was coated onto the outer layer of preformed biodegradable microcapsules consisting of sodium alginate and chitosan. The fabricated photosensitive microcapsules were characterized by optical microscopy, scanning electron microscopy, and confocal laser scanning microscopy. The assembled materials maintained intact spherical morphology and thus showed good ability to form thin films. Electron spin resonance spectroscopy allowed direct observation of the generation of singlet oxygen ($^1O_2$) from photosensitive microcapsules under light excitation at about 545 nm. Furthermore, with increasing light radiation, the content of $^1O_2$ increased, as detected by a chemical probe. In vitro cellular toxicity assays showed that RB-CHI-coated photosensitive microcapsules exhibit good biocompatibility in darkness and high cytotoxicity after irradiation, and could provide new photoresponsive drug-delivery vehicles.

Keywords: cancer · microcapsules · rose bengal · self-assembly · singlet oxygen

Introduction

Encapsulation of versatile photoactive species such as dyes, drugs, heterogeneous catalysts, and metal nanoparticles in nanoengineered carriers is becoming increasingly important for a wide variety of applications ranging from drug delivery to biomedicine and biotechnology.[1–3] Among these photoactive ingredients, photosensitized drugs or photosensitizers (PSs) capable of yielding cytotoxic singlet oxygen ($^1O_2$) have been widely explored in cell biology, photodynamic therapy, and blood sterilization.[4] However, many identified PS drugs and other photoactive small molecules used against cancer are poorly water soluble, and hence the PS efficacy is greatly reduced due to the aggregation of PS molecules in aqueous media.[5] To overcome this issue, diverse hydrophilic delivery vehicles such as gels, liposomes, and colloids were introduced to deliver encapsulated PSs at affected locations and thus enhance their photodynamic effects.[6–8] Recently, hydrophilic polyelectrolyte microcapsules, constructed by the layer-by-layer (LbL) self-assembly method,[9] have received particular attention as delivery vehicles for drug encapsulation and release due to their unique controllability of size, shape, and permeability, as well as large inner space capable of encapsulating drug molecules.[10,11] Some groups have applied microcapsules as photosensitive drug-delivery systems. Bédard et al.[12] prepared a remote laser-responsive system by incorporating *meso*-tetrakis(4-sulfonatophenyl)-porphin into microcapsule walls through an LbL self-assembly method. Li et al.[13] prepared hypocrellin B (HB)-accumulated microcapsules by loading water-insoluble, photosensitive HB into the interior of as-prepared microcapsules by a direct incubation process and found that HB-sensitized microcapsules exhibited high cytotoxicity after irradiation. In these systems, no qualitative or quantitative study on cytotoxic $^1O_2$ generated from PS-grafted photosensitive microcapsules was reported. Furthermore, PS drugs are distributed at random in polyelectrolyte wall materials or concentrated on the internal volume of capsules. As a result, as the concentration increases, aggregation of PSs occurs and results in radiationless deactivation and reduced efficiency in generating $^1O_2$.[14] Apart from this, encapsulated small-molecule PSs are prone to leak out of porous microcapsule walls unexpectedly before reaching the target region.[15] Considering these issues, we propose a new feasible solution in which PS molecules are first grafted to polymer chains to form conjugates through covalent attachment[16] for stable immobilization, and subsequently the resulting PS-grafted poly-

[a] X.-L. Wang, Y. Zeng, Dr. Y.-Z. Zheng, Prof. Dr. X. Tao
State Key Laboratory of Organic-Inorganic Composites
Beijing University of Chemical Technology
Beijing 100029 (P.R. China)
Fax: (+86) 10-64434784
E-mail: taoxia@yahoo.com

[b] Prof. Dr. J.-F. Chen
Research Center of the Ministry of Education for
High Gravity Engineering & Technology
Beijing University of Chemical Technology
Beijing 100029 (P.R. China)

[c] L.-X. Wang
Key Laboratory of Photochemistry, Institute of Chemistry
Chinese Academy of Sciences, Beijing 100080 (P.R. China)

[d] Y. Teng
Protein Science Core Facility Center, Institute of Biophysics
Chinese Academy of Sciences, Beijing 100101 (P.R. China)

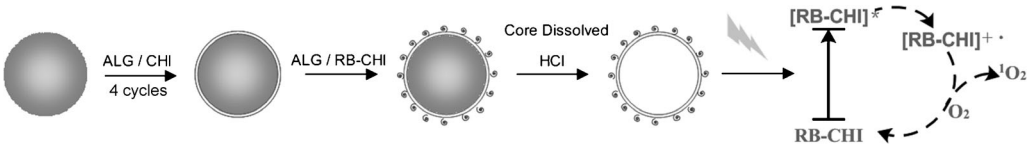

Scheme 1. Fabrication of photosensitive microcapsules by core-mediated LbL technique and generation of singlet oxygen.

mers, as one microcapsule wall component, are assembled onto microcapsules for specific accumulation of PSs and photoinduced generation of cytotoxic $^1O_2$.

Biodegradable microcapsules composed of sodium alginate (ALG)/chitosan (CHI) have been shown to be a promising vehicle for loading and controlled release of drugs. In this work, we fabricated novel photosensitive microcapsules by an LbL self-assembly technique in which rose bengal (RB), a potent PS, was first grafted to CHI chains through a stable chemical bond, followed by alternating assembly of ALG and CHI/RB-grafted CHI (RB-CHI) on dissolvable templates and subsequent removal of cores (Scheme 1). Generation of $^1O_2$ by the resultant photosensitive microcapsules on exposure to light of appropriate wavelength was investigated by ESR spectroscopy and a chemical approach. The phototoxic effects of photosensitive microcapsules and polymeric RB-CHI on human breast adenocarcinoma (MCF-7) cells on irradiation were studied, and cell viability was estimated in 3-(4,5-dimethylthiazol-2-yl)-2,5-diphenyltetrazolium bromide (MTT) assays.

Results and Discussion

Polymeric photosensitizer RB-CHI: To convert the OH group of the acid moiety of RB to a good leaving group prior to treatment with the amino group of CHI, EDC, and NHS were added to the reaction system to activate the carboxylic acid, and FTIR spectra were recorded to confirm chemical linkage between CHI and RB. Figure 1 shows transmittance spectra and corresponding characteristic peaks of CHI and RB-CHI in the solid state. Before grafting, weak peaks at 1655 and 1599 cm^{-1} can be ascribed to C=O and NH_2 groups of CHI.[16b] After RB was grafted to CHI, the original 1599 cm^{-1} peak decreased sharply and concomitantly two characteristic peaks at 1643 and 1548 cm^{-1}, corresponding to C=O stretching vibration (amide band I) and NH bending and CN stretching (amide band II), respectively, appeared.[17]

Besides, a new strong absorbance peak appeared at about 1450 cm^{-1} and can be ascribed to CN stretching.[18] Also, no peak at about 1730 cm^{-1} assignable to the CO stretching vibration of the ester units occurred, that is, amino groups of CHI as effective binding sites can be grafted to carboxyl groups of RB in a dehydration reaction,[16b] though a previous report demonstrated that the reaction between the hydroxyl groups of CHI and the carboxyl groups of RB can occur to some extent.[19]

Possible changes in binding energies of C, O, N, and I species due to RB grafting were investigated by X-ray photoelectron spectroscopy (XPS). Figure 2 shows survey spectra

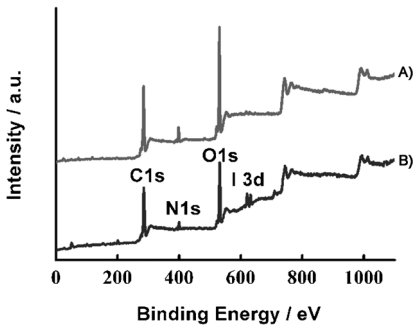

Figure 2. XPS survey scans for CHI (A) and RB-CHI (B), and the elemental compositions excluding hydrogen; atom% for C 1s: 64.77 (CHI), 68.84 (RB-CHI); for O 1s: 29.17 (CHI), 25.51 (RB-CHI); for N 1s: 6.06 (CHI), 4.89 (RB-CHI); for I 3d: not recorded (CHI), 0.76 (RB-CHI).

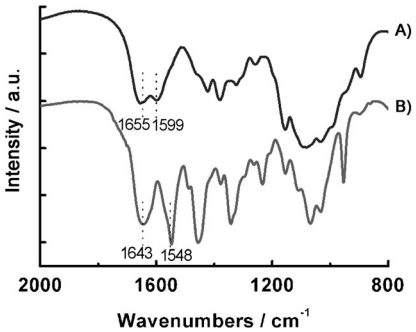

Figure 1. FTIR spectra of CHI (A) and RB-CHI (B). Peaks at 1655 and 1599 cm^{-1} are ascribed to C=O and NH_2 groups of CHI, and peaks at 1643 and 1548 cm^{-1} to amide bands I and II of RB-grafted CHI.

of CHI before and after RB grafting. Compared to the spectrum of CHI, the wide-scan spectrum of RB-CHI exhibits a new double peak around 620.5 and 631.8 eV characteristic of I 3d, and the contributions of C 1s, N 1s, and O 1s components in RB-CHI showed changes from 64.77 to 68.84%, from 6.06 to 4.89%, and from 29.17 to 25.51%, respectively, because of introduction of RB. In addition, the substitution ratio was estimated from atomic contents of the elements in RB-CHI to be about 3.90 mol% with respect to the glucosamine unit of CHI. Core-level spectra with fitted peaks of CHI and RB-CHI are shown in Figure 3. For RB-CHI, the C 1s core-level spectra can be curve-fitted with peak components of 285.8 eV for CN species and at 287.4 eV for CONH species,[20] which compare to peaks of CHI at 286.2 eV for

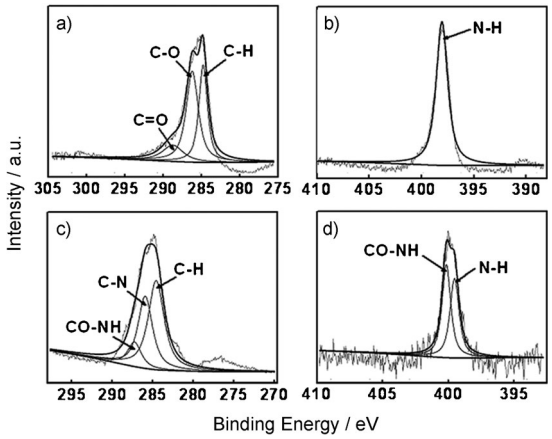

Figure 3. XPS core-level scans for the C 1s (a) and N 1s spectral regions (b) of CHI as well as the C 1s (c) and N 1s (d) spectral regions of RB-CHI.

C–O species and at 288.3 eV for C=O species.[21] By comparison to the N 1s spectrum of CHI containing a sole peak component for primary amine, the N 1s core-level spectrum of RB-CHI consists of two peaks at 399.4 and 400.2 eV, which are assigned to amine nitrogen and amide nitrogen, respectively, in excellent agreement with the previously reported XPS investigation.[22] In light of these results and discussion above, one can reasonably conclude that RB has been successfully grafted to CHI.

Morphology of photosensitive microcapsules: Preliminary morphological studies on $(ALG/CHI)_4$/ALG/RB-CHI photosensitive microcapsules were conducted under an optical microscope. The constructed microcapsules exhibit good dispersity, spherical shape, and uniform size (ca. 3 μm in diameter), as shown in Figure 4a. Figure 4b shows an overview

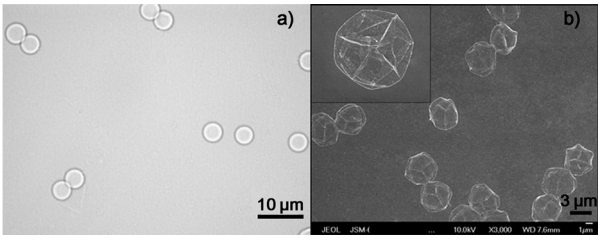

Figure 4. Optical micrograph (a) and SEM image (b) of photosensitive microcapsules. Inset shows a high-resolution SEM image of hollow $(ALG/CHI)_5$.

SEM image of air-dried photosensitive microcapsules exhibiting many folds and creases in flat disklike microcapsules. In contrast to $(ALG/CHI)_5$ capsules (inset of Figure 4b), RB-CHI coated photosensitive microcapsules show slight morphological changes. The RB moiety of the RB-CHI wall component is an iodine derivative of fluorescein with fluorescence, and thus the constructed $(ALG/CHI)_4$/ALG/RB-CHI capsules can be traced by CLSM observations. Figure 5a shows many vivid red fluorescent rings along the perimeter of the photosensitive capsules with outermost RB-CHI coat as wall component. This phenomenon demon-

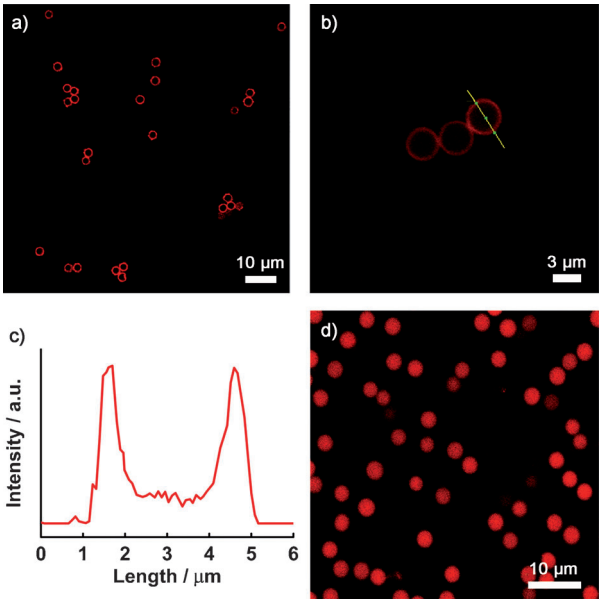

Figure 5. CLSM images of $(ALG/CHI)_4$/ALG/RB-CHI capsules (a), fluorescence intensity of $(ALG/CHI)_4$/ALG/RB-CHI capsules collected along the line (b and c), and $(ALG/CHI)_5$ capsules loaded with free RB (d). Excitation at 543 nm.

strates directly that RB-CHI is immobilized on the exterior of microcapsules as a polymeric photosensitizer. To investigate the fluorescence intensity from the microcapsule wall, a line was drawn across the microcapsule center (Figure 5b). The fluorescence distribution profile along the line shows two equal-intensity fluorescence peaks mainly concentrated on the outer wall of the capsule at a separation corresponding to the microcapsule diameter (Figure 5c). In addition, we carried out a control experiment by directly loading free RB in the $(ALG/CHI)_5$ suspension by a incubation process, and found that free RB molecules could also migrate across the capsule walls and then accumulate inside the microcapsules, which exhibit a red fluorescent region in their entire interior (Figure 5d). This also further suggests that pregrafting RB to CHI is a key to fabricating hollow photosensitive microcapsules, and leaves plenty of room to encapsulate active species in the microcapsule interiors.

Detection of singlet oxygen: Stable nitroxide radical TEMPO, detectable by ESR, was implicated in the reaction of TEMP with $^1O_2$ formed by PSs (see Scheme 2), whereby TEMP was used as a probe molecule, and TEMPO is a TEMP–$^1O_2$ spin adduct.[23] As shown in the inset of Figure 6, when an aqueous suspension containing photosensitive microcapsules and TEMP was irradiated at room temperature, a typical triplet signal characteristic of TEMPO appeared, while without irradiation there was no signal. This provides the diagnostics for $^1O_2$ generated from photosensitive micro-

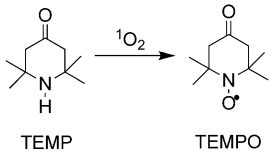

Scheme 2.

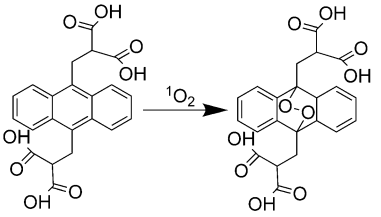

Scheme 3.

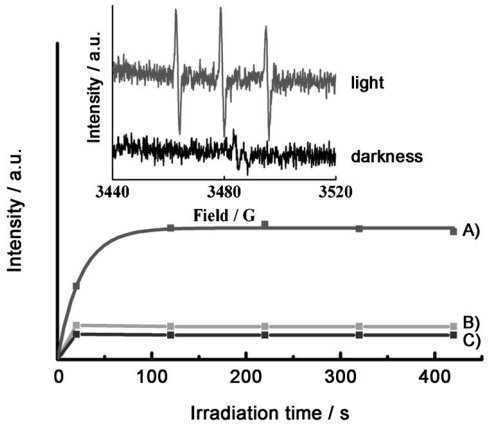

Figure 6. Changes of ESR signal intensity caused by the production of the spin adduct of TEMPO during illumination of TEMP in photosensitive capsules (A), photosensitive capsules with quencher histidine (B), and hollow capsules (C). Inset showing ESR signals of TEMPO with or without irradiation.

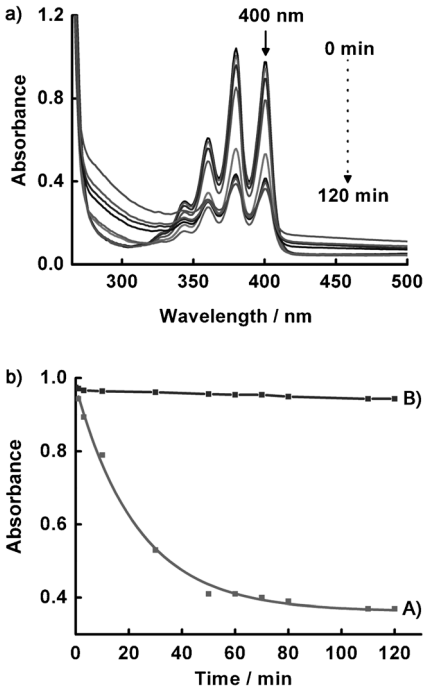

Figure 7. a) Absorption spectra of ABDA in the presence of $(ALG/CHI)_4$/ALG/RB-CHI capsules under irradiation over different periods of time. b) Absorbance changes of ABDA caused by $^1O_2$ oxidation plotted against irradiation time in the presence (A) and absence (B) of photosensitive capsules.

capsules. Furthermore, with increasing irradiation time, ESR signal intensities from photosensitive microcapsules initially increased at a fast rate and reached a stable plateau in a short period (Figure 6; curve A). To further verify that $^1O_2$ is involved in the photosensitizing process, we carried an experiment in which histidine was added as $^1O_2$ quencher to the photosensitive microcapsule system. In the presence of histidine, the signal intensities were dramatically suppressed just like those of the hollow capsules (Figure 6; curve B and curve C), in agreement with previous reports.[24] This confirms that TEMPO is formed by reaction of TEMP with $^1O_2$ generated from photosensitive microcapsules on irradiation.

Besides ESR detection, a chemical method based on water-soluble 9,10-anthracenediylbis(methylene)dimalonic acid (ABDA) detector was also employed to investigate the photogeneration process and the quantum yield of $^1O_2$ from RB-CHI-coated capsules by monitoring the loss of absorbance intensity of ABDA at 400 nm.[25] ABDA has a high reaction rate constant with $^1O_2$ and can yield a steady-state endoperoxide for UV detection (see Scheme 3). The loss of absorbance intensity at 400 nm of ADBA in a photosensitive microcapsule suspension with increasing exposure time is shown in Figure 7a. Under irradiation, the characteristic absorption band of ADBA at approximately 400 nm decreased rapidly within the initial 40 min, showed slow photobleaching with further irradiation, and finally remained unchanged after 120 min. The time-dependent decrease of ABDA indicated an increased amount of $^1O_2$ produced by RB-CHI-coated capsules (Figure 7b). The photobleaching rate of ABDA in the presence of photosensitive microcapsules follows a first-order exponential decay function dependent on exposure time with a coefficient of determination of $R^2 = 0.9966$ (Figure 7b, curve A). In contract, a control experiment showed that pure ABDA was bleached to a small extent in the absence of photosensitive microcapsules (Figure 7b, curve B), that is, photobleaching of ABDA is caused by oxidation of $^1O_2$ generated from photosensitive microcapsules instead of its photoreaction in the excited state.[25] By using RB as reference ($\Phi_{RB} = 0.75$[26]), the $^1O_2$ quantum yield of RB-CHI-coated capsules was calculated to be as high as 0.38 according to the method reported in the literature,[16b,27] and this value seems reasonable because it lies in the broad range of quantum yields from 0.05 to 0.75 for RB-grafted polymers.[28]

Cytotoxicity: Once the photosensitive microcapsules were verified to be capable of generating $^1O_2$, we studied cell phototoxicity to MCF-7 cells in vitro using the MTT assay to assess their photoresponsive therapeutic action.[29] Incubation of RB-CHI-coated photosensitive capsules with the cells was followed by light illumination. Cells that were normally incubated with capsules in the dark or that were incubated only in the cell culture medium under irradiation were employed as controls. Cell death after irradiation (69%) increased sharply in the presence of RB-CHI-coated photosensitive capsules compared to the uniform solution of RB-CHI with lower toxicity of 52% ($p < 0.01$), as shown in Figure 8. This result could be explained by the fact that

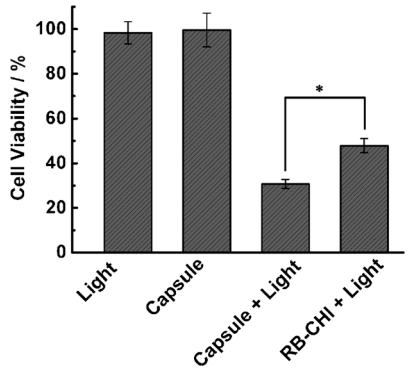

Figure 8. Percentage viability of MCF-7 cells under various conditions. a) Treatment with light. b) Photosensitive capsules in the dark. c) Photosensitive capsules under light. d) RB-CHI solution under light. Asterisks denote the significant differences with $p < 0.01$. (values: mean ± standard deviation of five replicates).

MCF-7 cells are attached, and sedimentation of photosensitive microcapsules provided a more dramatic interaction, a larger contact area, and a shorter reaction distance for short-lived $^1O_2$. To further verify whether interaction of cancer cells with RB-CHI-coated capsules occurred, the CLSM technique was employed. Figure 9, left, showed irregular-shaped red fluorescence in the marked positions, that is, RB-CHI-coated capsules can be captured by cells after incubation. Confocal section micrographs in the z direction further revealed that fluorescence completely originated from the cell-incorporated capsules. The capsules internalized through phagocytosis could also be distinctly observed in the bright-field image (Figure 9, right). The RB-CHI-coated photosensitive capsules generated sufficient $^1O_2$ to kill tumor cells. The mechanism of $^1O_2$ generation from RB-CHI coatings in a photodynamic process is summarized in Scheme 1. Control experiments showed that the irradiation used in this phototoxicity study has no effect on cell growth and the photosensitive microcapsules prepared in the dark have relatively high viability, as expected ($p < 0.01$). This exceptional biocompatibility will make the photosensitive microcapsules ideal delivery vehicles for drug loading and release.

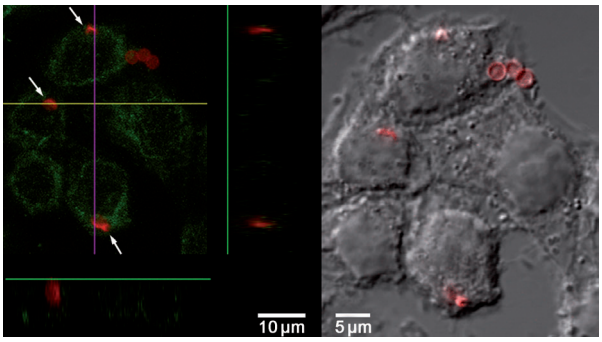

Figure 9. CLSM images showing RB-CHI-coated capsules taken up by MCF-7 cells. Left: Fluorescence images of the interaction of cells and capsules. The xz orthogonal section images at the bottom and on the right were recorded along the yellow and purple cross lines, respectively. Right: Bright-field image of cells after incubation with RB-CHI-coated capsules. The microtubules of the cells were labeled with FITC (green) and RB-CHI-coated capsules were preloaded with free RB for clear observation (red).

Conclusion

We have reported the synthesis of polymeric photosensitizer RB-CHI and their implementation as a wall component of biodegradable, photosensitive microcapsules with uniform size and good dispersity in aqueous solution. On irradiation with light of appropriate wavelength, the microcapsules efficiently generate $^1O_2$. In vitro cytoxicity tests showed that RB-CHI-functionalized capsules photoinduced significant cell death compared to free RB-CHI, while the microcapsules themselves are biocompatible with cells in the dark. We expect that highly active PSs other than RB can be grafted to biopolymers and then assembled on microcapsules. The fabricated photofunctional hollow microcapsules may also offer plenty of inner space to load active species such as cancer drugs for potential combination therapy in patients.

Experimental Section

Materials: Melamine–formaldehyde (MF, ca. 3 µm) particles were prepared by previously described dispersion polymerization method.[30] ALG (M_w 12000–80000 kDa) was obtained from Sigma, Canada. CHI (M_w 30000 kDa, degree of deacetylation >94.5%) was obtained from Primex Biochemicals, Norway. 1-Ethyl-3-(3-dimethyllaminopropyl) carbodiimide hydrochloride (EDC, 98.5%) and *N*-hydroxysuccinimide (NHS, 98.0%) were obtained from Alading Agents. RB (ca. 99.0%), 3-(4,5-dimethylthiazol-2-yl)-2,5-diphenyltetrazolium bromide (MTT), 2,2,6,6-tetramethyl-4-piperidone (TEMP, 99.0%), and 9,10-anthracenediylbis(methylene)dimalonic acid (ABDA, 90.0%) were purchased from Sigma. MCF-7 cell line was generously donated by the ATCC. All other chemicals used in the experiments were obtained from commercial sources as analytical reagents and used without further purification. Millipore water with a resistivity of 18.2 $M\Omega\,cm^{-1}$ reduced by a reagent water system (Easy pure, Barnstead) was used throughout the study. The chemical structures of RB as well as the polyelectrolytes used for the fabrication of the capsules are given below.

Preparation of RB-CHI: The general procedure with a 4:1 molar ratio of the glucosamine unit of CHI to RB is briefly summarized.[16b,31] 0.1 g of

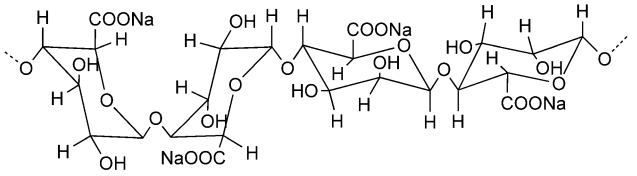

Alginate sodium (ALG)

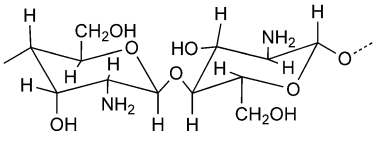

Chitosan (CHI)

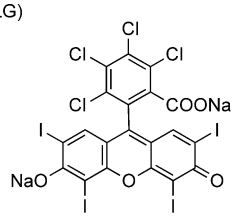

Rose bengal (RB)

CHI was dissolved in 1% acetic acid (10 mL) and the solution stirred for more than 10 h. Then 0.48 g EDC was added to a solution of RB (15 mg, 15 mM) in methanol to activate the carboxyl group for 5 min followed by NHS stabilization for further 20 min, with a 4:1 molar ratio of EDC to NHS. Subsequently, the solution of CHI with pH adjusted to 5.8 was added dropwise over a period of 20 min and reacted with RB under intense stirring at room temperature overnight. The mixture was further purified by dialysis and wash/centrifugation circles until no free RB was detected in the supernatant. After freeze-drying, RB-CHI was isolated as a pink powder.

Fabrication of photosensitive hollow microcapsules: Polyelectrolyte microcapsules were fabricated by using weakly polymerized MF cores as removable templates due to their stable monodispersity with uniform diameter and high density of surface charges.[32] General procedure for capsule fabrication is summarized: 1 mL of ALG (1 mg mL^{-1} in 0.5 M NaCl) or CHI solution (1 mg mL^{-1} in 0.2 M NaCl, pH 3.3) with opposite charge to MF templates (15 mg mL^{-1}) or the last layer was assembled through electrostatic interaction. Each layer was left to absorb for one hour with dispersion at intervals, and the excess species was removed by three centrifugation (2500 *g*, 3 min)/washing/redispersion cycles with Millipore water. On the outmost layer, RB-CHI was employed as photosensitive coating in place of CHI. Then MF templates were dissolved in a solution of hydrochloric acid (pH 1), after which centrifugation and washing with Millipore water were carried out for the construction of hollow photosensitive microcapsules with composition $(ALG/CHI)_4(ALG/RB\text{-}CHI)$. The concentration of photosensitive microcapsules used throughout the study was 5×10^7 microcapsules per milliliter, as determined by using a blood-cell counting chamber, if not otherwise indicated. The overall fabrication procedure is summarized in Scheme 1.

Detection of singlet oxygen: To identify $^1O_2$ production, the ESR technique was employed. Spin trap TEMP reacts with $^1O_2$ forming stable nitroxyl radical spin adduct TEMPO, which produces a triplet ESR signal. Photoinduced ESR spectra were obtained by mixing 40 μL of 2.0 M TEMP with 150 μL of photosensitive microcapsule suspension for immediate ESR analysis. Hollow microcapsules and histidine/photosensitive microcapsules were used as controls. As $^1O_2$ quencher, 40 μL of 10 mM histidine prepared in phosphate-buffered saline (PBS, pH 7.4) was added to the microcapsule system. Besides, the ESR signals of TEMPO generated by photosensitive microcapsules in the presence of TEMP with or without irradiation were collected.

A chemical oxidation method based on ABDA was also used to assess the capability of photosensitive microcapsules to generate $^1O_2$. Water-soluble ABDA exhibits photobleaching when oxidized by $^1O_2$ to its endoperoxide, which causes a decrease in ABDA absorption at 400 nm (maximum absorbance of ABDA). In this method, a suspension of photosensitive microcapsules (3 mL in PBS, pH 7.4) containing 50 μL of 10 mM ABDA was irradiated with a 500 W halogen lamp through a 545 nm cutoff filter. The control experiment was carried out with 10 mM ABDA solution and the same irradiation but in the absence of photosensitive microcapsules. The change in ABDA absorption at 400 nm was recorded as a function of irradiation time. Furthermore, the $^1O_2$ quantum yield of photosensitive microcapsules was measured according to Equation (1), where Φ is the quantum yield of $^1O_2$ and K is the slope of the bleaching curve, R denotes reference, and S the sample.

$$\Phi_S = \Phi_R \frac{K_S}{K_R} \quad (1)$$

Cell culture: For routine maintenance, MCF-7 cells were cultured in Dulbecco's modified Eagle's medium (DMEM, Gibco BRL) containing high glucose, 10% fetal bovine serum, and 1% gentamicin at 37 °C in a humidified atmosphere of 5% CO_2. The medium was renewed every day and passage was conducted when confluent by trypsinization of the mixture containing 0.25% trypsin and 0.02% ethylenediaminetraacetic acid. Sterile culture technique was used in all manipulations done to cells.

In vitro phototoxicity of photosensitive microcapsules to MCF-7 cells: MCF-7 cells in aliquots (2.0×10^5 cells per well) seeded on 96-well plates were cultured in CO_2 incubator for 24 h for cell attachment. Then the cells were exposed to different samples, that is, photosensitive microcapsules, and RB-CHI solution, after refreshing the culture medium. For each sample, the absolute amount of PS moiety (7 μg mL^{-1} chromophore) was maintained equivalent. After 6 h of further incubation, one plate was irradiated with a 500 W halogen lamp through a 545 nm cutoff filter for 20 min with a central optical density of 13 mW cm^{-2}, measured by a photometer (ILT, 1400A). At the same time, the other sample was kept under the same conditions except for irradiation. Subsequently both plates were cultured for a further 16 h for cells to interact with the additives adequately, after which the MTT assay was employed to assess the viability of cells. In a typical MTT method, 50 μL of MTT solution (1 mg mL^{-1} in PBS, pH 7.4) was added into each well for four-hour incubation, and then 150 μL of dimethyl sulfoxide solution was added to the cells after removal of all other media. Absorbance at 570 nm was recorded on a microplate reader (Bio-Rad-318, Molecular Devices, Sunnyvale, CA) to estimate the proportion of viable cells. The cell viability was assessed as the percentage of viable treated cells compared to the cells incubated at normal state without treatment by irradiation or any agent. Interaction of live cells and capsules was traced by first labeling cells with fluorescein isothiocyanate (FITC) at 10 μg mL^{-1} for 1 h at 37 °C, and then incubating with capsules for 16 h. Excess fluorophore and unchanged capsules were removed by washing with PBS three times for 5 min.

Instrumentation and measurements: FTIR spectra were recorded on a Bruker Vector-22 IR spectrometer by using the KBr pellet method, and the accessory software supplied with the spectrometer was used to process the data. XPS analysis of RB-CHI was conducted on a ThermoFish Scientific ESCALAB250 spectrometer with an $Mg_{K\alpha}$ anode (300 W). A passing energy of 200 eV at intervals of 1.0 eV for survey scans and of 30 eV at intervals of 0.05 eV for high-resolution scans was used with the neutral C 1s peak at 284.6 eV serving as a standard for all other binding energies (BEs).[20] To obtain accurate results, sensitivity factors were employed to correct the intensity of tested components, and then the relative molar percentage was calculated. UV/Vis spectroscopy was performed on a Shimadzu UV 2501 spectrometer. Fluorescent images were obtained by using an Olympus FV500 confocal laser scanning microscope (CLSM) excited at a wavelength of 543 nm. ESR spectra were taken on a Bruker EPR E-500 spectrometer. SEM images were collected on a JEOL JSM-6701-F microscope to study the morphology of the prepared samples. The concentrations of microcapsules and MCF-7 cells were counted in a blood-cell counting chamber. A 500 W halogen lamp with a 545 nm cutoff filter was used as irradiation source.

Acknowledgements

This work was financially supported by NSFC (Nos. 20906004, 20977005, 20821004).

[1] a) X. Tao, J. Li, H. Möhwald, *Chem. Eur. J.* **2004**, *10*, 3397–3403; b) Z. F. Dai, L. Dähne, E. Donath, H. Möhwald, *J. Phys. Chem. B* **2002**, *106*, 11501–11508; c) M. Bédard, A. G. Skirtach, G. B. Sukhorukov, *Macromol. Rapid Commun.* **2007**, *28*, 1517–1521.

[2] a) T. S. Balaban, A. D. Bhise, M. Fischer, M. Linke-Schaetzel, C. Roussel, N. Vanthuyne, *Angew. Chem.* **2003**, *115*, 2190–2194; *Angew. Chem. Int. Ed.* **2003**, *42*, 2140–2144; b) T. Joki, M. Machluf, A. Atala, J. Zhu, N. T. Seyfried, I. F. Dunn, T. Abe, R. S. Carroll, P. M. Black, *Nature Biotechnol.* **2001**, *19*, 35–39.

[3] a) A. S. Angelatos, B. Radt, F. Caruso, *J. Phys. Chem. B* **2005**, *109*, 3071–3076; b) M. F. Bédard, D. Braun, G. B. Sukhorukov, A. G. Skirtach, *ACS Nano* **2008**, *2*, 1807–1816; c) Y. Klichko, M. Liong, E. Choi, S. Angelos, A. E. Nel, J. F. Stoddart, F. Tamanoi, J. I. Zink, *J. Am. Ceram. Soc.* **2009**, *92*, S2–S10.

[4] a) I. J. Macdonald, T. J. Dougherty, *J. Porphyrins Phthalocyanines* **2001**, *5*, 105–129; b) M. C. DeRosa, R. J. Crutchley, *Coord. Chem. Rev.* **2002**, *233–234*, 351–371; c) M. R. Hamblin, T. Hasan, *Photochem. Photobiol. Sci.* **2004**, *3*, 436–450.

[5] J. P. Keene, D. Kessel, E. J. Land, R. W. Redmond, T. G. Truscott, *Photochem. Photobiol.* **1986**, *43*, 117–120.

[6] H. Y. Lee, Z. X. Zhou, S. Chen, M. H. Zhang, T. Shen, *Dyes Pigm.* **2006**, *68*, 1–10.

[7] T. Wu, S. J. Xu, J. Q. Shen, A. M. Song, S. Chen, M. H. Zhang, T. D. Shen, *Anticancer Drug Design* **2000**, *15*, 287–293.

[8] S. J. Xu, S. Chen, M. H. Zhang, S. Tao, Y. P. Zhao, Z. W. Liu, Y. D. Wu, *Biochim. Biophys. Acta* **2001**, *1537*, 222–232.

[9] S. W. Keller, S. A. Johnson, E. S. Brigham, E. H. Yonemoto, T. E. Mallouk, *J. Am. Chem. Soc.* **1995**, *117*, 12879–12880.

[10] X. Tao, J. M. Su, J. F. Chen, *Chem. Eur. J.* **2006**, *12*, 4164–4169.

[11] a) J. M. Su, X. Tao, H. Xu, J. F. Chen, *Polymer* **2007**, *48*, 7598–7603; b) X. Tao, J. M. Su, J. F. Chen, J. Zhao, *Chem. Commun.* **2005**, 4607–4609; c) Q. H. Zhao, S. Zhang, W. J. Tong, C. Y. Gao, J. C. Shen, *Eur. Polym. J.* **2006**, *42*, 3341–3351.

[12] M. F. Bédard, S. Sadasivan, G. B. Sukhorukov, A. Skirtach, *J. Mater. Chem.* **2009**, *19*, 2226–2233.

[13] K. W. Wang, Q. He, X. H. Yan, Y. Cui, W. Qi, L. Duan, J. B. Li, *J. Mater. Chem.* **2007**, *17*, 4018–4021.

[14] M. Mirenda, L. E. Dicelio, E. S. Román, *J. Phys. Chem. B* **2008**, *112*, 12201–12207.

[15] S. Tomita, K. Sato, J. Anzai, *Mater. Sci. Eng. C* **2009**, *29*, 2024–2028.

[16] a) V. Chiono, P. Gentile, F. Boccafoschi, I. Carmagnola, M. Ninov, V. Georgieva, G. Georgiev, G. Ciardelli, *Biomacromolecules* **2010**, *11*, 309–315; b) L. Moczek, M. Nowakowska, *Biomacromolecules* **2007**, *8*, 433–438; c) M. Nowakowska, L. Moczek, K. Szczubiałka, *Biomacromolecules* **2008**, *9*, 1631–1636.

[17] a) S. Y. Lin, K. S. Chen, R. C. Liang, *Polymer* **1999**, *40*, 2619–2624; b) A. Percot, X. X. Zhu, M. Lafleur, *J. Polym. Sci. Part B* **2000**, *38*, 907–915.

[18] D. Q. Li, B. I. Swanson, J. M. Robinson, M. A. Hoffbauer, *J. Am. Chem. Soc.* **1993**, *115*, 6975–6980.

[19] X. Qu, A. Wirsén, A. C. Albertsson, *J. Appl. Polym. Sci.* **1999**, *74*, 3193–3202.

[20] L. Ying, E. T. Kang, K. G. Neoh, *Langmuir* **2002**, *18*, 6416–6423.

[21] F. Geneste, C. Moinet, S. Ababou-Girard, F. Solal, *New J. Chem.* **2005**, *29*, 1520–1526.

[22] a) J. Charlier, V. Detalle, F. Valin, C. Bureau, G. J. Lecayon, *J. Vac. Sci. Technol. A* **1997**, *15*, 353–364; b) A. J. Wagner, G. M. Wolfe, D. H. Fairbrother, *Appl. Surf. Sci.* **2003**, *219*, 317–328.

[23] a) Y. Lion, M. Delmelle, A. van de Vorst, *Nature* **1976**, *263*, 442–443; b) J. Moan, E. Wold, *Nature* **1979**, *279*, 450–451.

[24] a) R. D. Hall, C. F. Chignell, *Photochem. Photobiol.* **1987**, *45*, 459–464; b) H. Yuying, A. Jingyi, J. Lijin, *Free Radical Biol. Med.* **1999**, *26*, 1146–1157.

[25] a) I. Roy, T. Y. Ohulchanskyy, H. E. Pudavar, E. J. Bergey, A. R. Oseroff, J. Morgan, T. J. Dougherty, P. N. Prasad, *J. Am. Chem. Soc.* **2003**, *125*, 7860–7865; b) B. A. Lindig, M. A. J. Rodgers, A. P. Schaap, *J. Am. Chem. Soc.* **1980**, *102*, 5590–5593.

[26] a) E. Gandin, Y. Lion, A. Van de Vorst, *Photochem. Photobiol.* **1983**, *37*, 271–278; b) P. Murasecco-Suardi, E. Gassmann, A. M. Braun, E. Oliveros, *Helv. Chim. Acta* **1987**, *70*, 1760–1773.

[27] a) A. P. Schaap, A. L. Thayer, E. C. Blossey, D. C. Neckers, *J. Am. Chem. Soc.* **1975**, *97*, 3741–3745; b) Y. Vakrat-Haglili, L. Weiner, V. Brumfeld, A. Brandis, Y. Salomon, B. Mcllroy, B. C. Wilson, A. Pawlak, M. Rozanowska, T. Sarna and A. Scherz, *J. Am. Chem. Soc.* **2005**, *127*, 6487–6497.

[28] a) M. Nowakowska, M. Kępczyński, M. Dąbrowska, *Macromol. Chem. Phys.* **2001**, *202*, 1679–1688; b) M. Nowakowska, M. Kępczyński, K. Szczubialka, *Pure Appl. Chem.* **2001**, *73*, 491–495.

[29] a) Y. J. Yang, X. Tao, Q. Hou, Y. Ma, X. L. Chen, J. F. Chen, *Acta Biomater.* **2010**, *6*, 3092–3100; b) A. Rosenfeld, J. Morgan, L. N. Goswami, T. Ohulchanskyy, X. Zheng, P. N. Prasad, A. Oseroff, R. K. Pandey, *Photochem. Photobiol.* **2006**, *82*, 626–634.

[30] Y. J. Liu, Y. H. Zhu, S. Q. Zhang, X. L. Yang, *J. Funct. Polym.* **2004**, *17*, 113–118.

[31] a) H. T. Deng, J. J. Wang, M. Ma, Z. Y. Liu, F. Zheng, *Chin. Chem. Lett.* **2009**, *20*, 995–999; b) S. Kwon, J. H. Park, H. Chung, I. C. Kwon, S. Y. Jeong, I. S. Kim, *Langmuir* **2003**, *19*, 10188–10193.

[32] Y. Ding, Y. Zhao, X. Tao, Y. Z. Zheng, J. F. Chen, *Polymer* **2009**, *50*, 2841–2846.

Received: March 30, 2011
Published online: August 18, 2011

